ARTICLES

Serum response factor regulates a muscle-specific microRNA that targets *Hand2* during cardiogenesis

Yong Zhao[1,2]†, Eva Samal[1,2]† & Deepak Srivastava[1,2]†

Gradients of signalling and transcription factors govern many aspects of embryogenesis, highlighting the need for spatiotemporal control of regulatory protein levels. MicroRNAs are phylogenetically conserved small RNAs that regulate the translation of target messenger RNAs, providing a mechanism for protein dose regulation. Here we show that microRNA-1-1 (miR-1-1) and miR-1-2 are specifically expressed in cardiac and skeletal muscle precursor cells. We found that the *miR-1* genes are direct transcriptional targets of muscle differentiation regulators including serum response factor, MyoD and Mef2. Correspondingly, excess *miR-1* in the developing heart leads to a decreased pool of proliferating ventricular cardiomyocytes. Using a new algorithm for microRNA target identification that incorporates features of RNA structure and target accessibility, we show that Hand2, a transcription factor that promotes ventricular cardiomyocyte expansion, is a target of miR-1. This work suggests that *miR-1* genes titrate the effects of critical cardiac regulatory proteins to control the balance between differentiation and proliferation during cardiogenesis.

Cellular differentiation and organogenesis involve restricted zones of transcriptional regulation that govern gene expression patterns during specific temporal windows. One mechanism for regulating the target genes activated by transcriptional regulators involves the dose-sensitive response of *cis* elements to gradients of DNA-binding proteins. In this scenario, differences in the levels of transcription factors result in the activation or repression of diverse target genes, allowing finer control of the spatial and temporal events of organogenesis.

MicroRNAs (miRNAs) mediate a recently recognized form of translational inhibition that alters the levels of critical regulators, thereby providing a mechanism for spatiotemporal control of developmental and homeostatic events across a wide range of plants and animals[1–3]. Genetic studies in *Caenorhabditis elegans* and *Drosophila melanogaster* suggest important functions for specific miRNAs in cell death and proliferation through direct interaction of miRNAs with target sequences in messenger RNAs[4–11]. However, understanding the specific roles of miRNAs and the regulatory pathways they control has been limited by a lack of reliable and specific methods for identifying miRNA targets.

The transcriptional regulation of cardiomyocyte differentiation and cardiogenesis is highly conserved and requires sequential activation and/or repression of different genetic programmes[12,13]. Early cardiomyocytes proliferate even as they begin to differentiate, but exit the cell cycle as differentiation progresses. Serum response factor (SRF) binds to CArG boxes in the regulatory region of numerous muscle-specific and growth-regulated genes, and thus has a dual role in regulating the balance between proliferation and differentiation during cardiogenesis[14–17]. Failure to maintain an adequate pool of undifferentiated myocyte precursors could result in organ hypoplasia, as observed in mice and zebrafish that lack the Hand transcription factor Hand2 (refs 18–23). Although dynamic temporal and spatial expression of regulatory pathway components is important in cardiogenesis, whether miRNAs are involved in refining cardiac transcriptional activity is unknown.

Here, we show that the cardiac and skeletal muscle-specific miRNA genes *miR-1-1* and *miR-1-2* are expressed in a chamber-specific manner during cardiogenesis and are activated during the period of differentiation. We find that both genes are direct targets of SRF and its potent co-activator myocardin, and that they are involved in negatively regulating ventricular cardiomyocyte proliferation[24]. We provide evidence that RNA accessibility is a principal feature of miRNA target recognition, and have incorporated this observation with cross-species sequence matching to identify *Hand2* as an evolutionarily conserved target of *miR-1*. This work reveals a new mechanism for regulating the balance between muscle differentiation and proliferation during organogenesis, and might provide a reliable and specific method for identification of microRNA targets.

miR-1 in developing cardiac and skeletal muscle

To determine whether miRNAs have a role in cardiac development or homeostasis, we searched for miRNAs that were expressed in the mouse cardiovascular system and were conserved across species ranging from flies to humans. On the basis of our *in silico* data and previous reports, the *miR-1* subfamily seemed to be cardiac-enriched[25,26]. The *miR-1* subfamily consists of two closely related miRNAs encoded by distinct genes that share near complete identity and are designated *miR-1-1* and *miR-1-2* (Fig. 1a). Northern blot analysis revealed that both *miR-1* genes were 21 base pairs (bp) in length and were expressed specifically in the heart and skeletal muscle of adult mice (Fig. 1b and Supplementary Fig. 1).

Owing to the similarity in the *miR-1-1* and *miR-1-2* sequences, and the small size of miRNAs, the relative expression of each *miR-1* gene could not be determined, nor could mRNA *in situ* hybridization

[1]Department of Pediatrics (Cardiology) and [2]Molecular Biology, University of Texas Southwestern Medical Center and Children's Medical Center Dallas, 6000 Harry Hines Boulevard, Dallas, Texas 75390-9148, USA. †Present address: Gladstone Institute of Cardiovascular Disease and Department of Pediatrics, University of California San Francisco, 1650 Owens Street, San Francisco, California 94158, USA.

© 2005 Nature Publishing Group

delineate the embryonic expression domains of the two genes. In order to define the tissue-specific expression and regulation of *miR-1* genes during embryogenesis, we searched for enhancers that might regulate *in vivo* transcription of *miR-1-1* or *miR-1-2*. Comparison of genomic sequences across species using rVISTA revealed that a 4.6 kilobase (kb) and 10.7 kb genomic region around *miR-1-1* and *miR-1-2*, respectively, was conserved between human and mouse (Fig. 1c). The 4.6 kb *miR-1-1* fragment was sufficient to direct lacZ expression in the hearts of transgenic mice after embryonic day (E)8.5 (Fig. 1d), with expression at the early stages being strongest in the inner curvature of the looping heart tube and atria. The inner curvature is less proliferative than the outer curvature, which expands and balloons ventrally to form the cardiac chambers. Cardiac expression of lacZ became more robust and uniform as cardiomyocyte differentiation proceeded, and expression in the myotome of somites also became apparent as skeletal muscle differentiation began (Fig. 1d). Similarly, the 10.7 kb *miR-1-2* fragment contained all the regulatory elements necessary to drive lacZ expression in the embryonic ventricles (but not the atria) and somites at stages corresponding to that described for *miR-1-1* (Fig. 1e). Both *miR-1* enhancers directed expression in the outflow tract of the heart, which arises from a secondary heart field[27], distinct from the primary heart field that contributes to atrial and left ventricular myocardium (Fig. 1d, e).

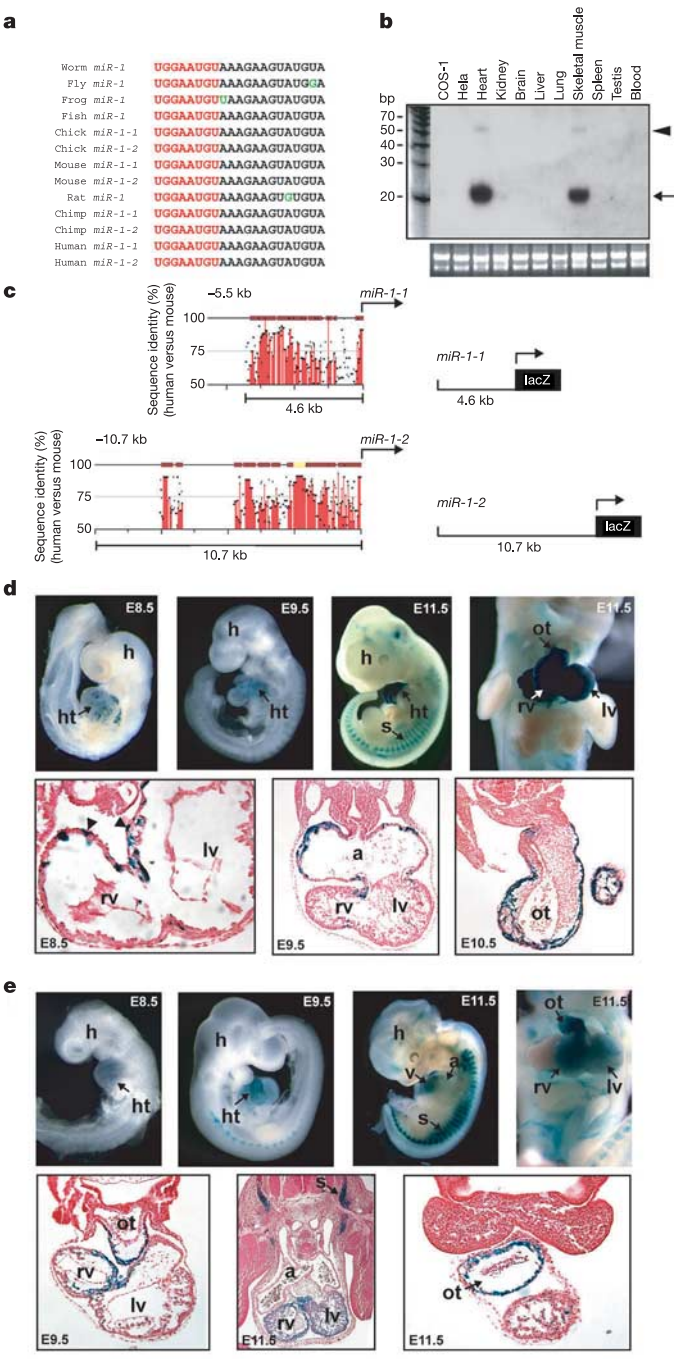

Figure 1 | *miR-1*s are highly conserved and are cardiac- and skeletal-muscle-specific. **a**, Sequence alignment of predicted *miR-1* genes from the indicated species. The eight 5′-nucleotides are highlighted in red; non-conserved residues are in green. **b**, Northern blot of multiple tissues hybridized using an miR-1-specific probe. The 70 bp unprocessed form (arrowhead) and 21 bp miR-1 (arrow) are indicated. **c**, Comparison of the *miR-1-1* and *miR-1-2* promoter regions between mouse and human. Percentage conservation of a 4.6 kb or 10.7 kb genomic region around *miR-1-1* or *miR-1-2* (respectively) is shown. **d**, **e**, Whole-mounts and sections showing embryonic expression of *miR-1-1* (**d**) or *miR-1-2* (**e**), shown by β-gal activity driven by the genomic fragments indicated in **c**. Arrowheads in **d** indicate the inner curvature. Abbreviations: a, atrium; h, head; ht, heart; lv, left ventricle; ot, outflow tract; rv, right ventricle; s, somites; v, ventricle.

SRF regulates *miR-1* in the heart

Deletion analyses of the *miR-1* enhancers suggested that a 2.6 kb and 0.35 kb region was sufficient for full *miR-1-1* and *miR-1-2* expression, respectively (Fig. 2a, b). Within these regions we noted several *cis* elements conserved between human and mouse that represented potential binding sites for the essential cardiac transcription factors Mef2, SRF, Nkx2.5 and Gata4. SRF sites in the *miR-1-1* and *miR-1-2* enhancers were nearly identical and highly conserved in human, mouse and chick, as were Mef2 sites in *miR-1-1* and MyoD sites in *miR-1-2* (Fig. 2c, d). In transgenic mice, the Mef2 site in the *miR-1-1* enhancer was dispensable for cardiac expression but was necessary for full somite regulation. Mutation of the *miR-1-1* SRF site abolished expression in the heart, and disruption of both the Mef2 and SRF sites abolished all activity of the enhancer (Fig. 2a). Consistent with a cardiac requirement for SRF, mutation of the SRF site in the *miR-1-2* regulatory region disrupted cardiac expression of *miR-1-2*, and mutation of the MyoD site only partially affected somitic expression (Fig. 2b).

In electromobility shift assays, SRF, Mef2 and MyoD could each specifically bind their respective sites in the *miR-1-1* and *mirR-1-2* enhancer regions (Fig. 2c, d). SRF is a weak activator of numerous muscle-specific genes and is thought to mediate muscle differentiation by regulating decisions of cellular proliferation and differentiation[14,15,28,29]. During cardiac and smooth muscle development, the SAP-domain protein myocardin serves as a potent co-activator for SRF and promotes muscle differentiation[24,30,31]. Consistent with this, we found that SRF was a weak activator of luciferase placed under the control of the *miR-1-1* or *miR-1-2* enhancers, but acted synergistically with myocardin to activate the *miR-1* gene enhancers (Fig. 2e and data not shown); myocardin activity was dependent on an intact SRF-binding site (Fig. 2e). Correspondingly, *miR-1* transcripts were undetectable in RNA from hearts lacking SRF through tissue-specific disruption of the *Srf* gene[28] (Fig. 2f). These data suggest that *miR-1-1* and *miR-1-2* function in SRF–myocardin-dependent pathways in cardiac progenitor cells, and are responsive to MyoD/Mef2 in skeletal muscle precursors.

miR-1 regulates ventricular cardiomyocytes

To determine whether the dosage of miR-1 target genes might be important in the SRF-dependent balance of proliferation and differentiation, we overexpressed miR-1 specifically in the developing heart under the control of the β-myosin heavy chain (MHC) promoter, which directs high levels of expression by E9.0. Overexpression of miR-1 resulted in developmental arrest at E13.5, secondary to thin-walled ventricles and heart failure (Fig. 3). The more proliferative compact zone in the *miR-1* transgenic embryos

© 2005 Nature Publishing Group

was only 3–5 cell layers thick, in contrast to non-transgenic littermates, which contained layers of 8–10 cells. Analysis of mitogenic activity using an antibody directed against phosphohistone H3 (Ser 10) revealed a significant decrease in the number of cycling myocardial cells in *miR-1* transgenic mice at E13.5 (Fig. 3), but no increase in apoptotic cells was observed (data not shown). Thus, a decrease in the protein levels of miR-1 targets during cardiogenesis resulted in a proliferation defect and failure of ventricular cardiomyocyte expansion. Given that *miR-1* expression is regulated by SRF and myocardin, this phenotype is consistent with premature differentiation and early withdrawal of myocytes from the cell cycle[16].

miR-1 targets *Hand2* mRNA

Genetic studies in flies and worms have identified several validated miRNA targets (Table 1). Recently, several computational methods have been developed for predicting miRNAs targets based on the fundamental assumption that the 5′-nucleotides of miRNAs are most critical for target recognition[32–37]. Although sequence-based predictions have been successful in plants, the algorithms used to date for non-plant miRNAs often result in few overlapping targets[34–38]. With few exceptions[39,40], large-scale predictions have not yet been validated by demonstration of miRNA activity on endogenous targets *in vivo*.

Target accessibility has long been established as an important factor for effective antisense oligonucleotide- and siRNA-mediated silencing[41], and we therefore postulated that it might also be involved in miRNA target repression. Using mFold, we analysed all miRNA targets identified to date and found that virtually all miRNA binding sites in 3′-UTRs were located in 'unstable' regions on the basis of free energy predictions (ΔG) and RNA structure. Table 1 lists the free

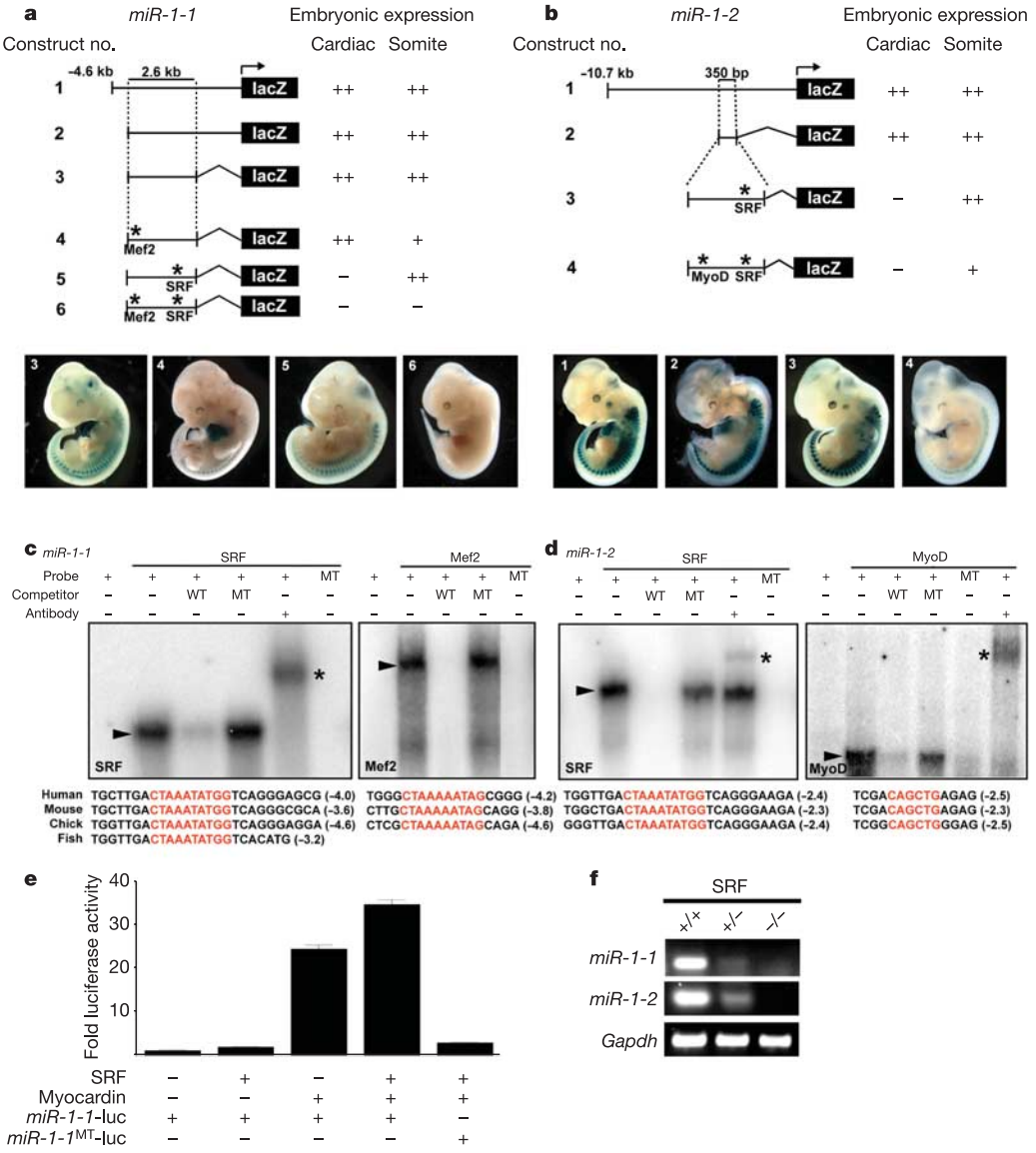

Figure 2 | SRF, Mef2 and MyoD directly regulate embryonic expression of *miR-1*. **a**, **b**, Deletion and mutation analyses of upstream enhancers of *miR-1-1* (**a**) or *miR-1-2* (**b**). A summary of the effects of mutations (asterisks) on cardiac or somite expression is presented. The bottom panel shows representative images, with construct numbers indicated. **c**, **d**, Electrophoretic mobility-shift assay using radiolabelled probes (wild type (WT) or mutant (MT)) for SRF, Mef2 or MyoD binding sites (arrowheads). Asterisk indicates supershift in the presence of antibody. Cross-species conservation of binding sites (with distance upstream of *miR-1*) is shown under the blots. **e**, Fold activation of luciferase downstream of the *miR-1-1* enhancer in COS1 cells by SRF and myocardin with or without a point mutation (MT) in the SRF-binding site. Error bars indicate standard deviations. **f**, PCR with reverse transcription (RT–PCR) of *miR-1* expression in hearts from mice heterozygous or homozygous for cardiac-specific disruption of SRF.

© 2005 Nature Publishing Group

energy of the flanking 70 nucleotides 3′ and 5′ of the (one or more) predicted miRNA target sequence(s) in the 3′-UTR of validated target genes. The ΔG of the 5′ or 3′ flanking region around at least one of the predicted miRNA binding sites within the 3′-UTR of each target gene was significantly lower than the average ΔG of 60 random 3′-UTRs (70 bp each) in the corresponding species (Table 1). This suggests a locally linear RNA structure around the target mRNA-binding site that cannot not form tight stems.

However, genes that had multiple putative binding sites typically had several sites that were in regions of high ΔG. To resolve this discrepancy, we compared the conservation of high ΔG versus low ΔG sites in closely related worm ($n = 3$) or fly ($n = 8$) species in an attempt to better predict the validity of true target sites (see Supplementary Fig. 2). We found that virtually all high ΔG sites had sequence differences in the critical 5′ region of the miRNA, several of which would clearly disrupt interaction, as seen in *lin-14* (site VI for lin-4 binding) and *lin-57* (site II for let-7 binding), making it unlikely that such sites are true targets (see Supplementary Fig. 2). In contrast, every low ΔG site was absolutely conserved across all species, consistent with the idea that they might represent actual target sites (see Supplementary Fig. 2). Consistent with the cross-species data, previous deletion of high ΔG sites in *lin-41* (sites III–VI for let-7 binding) suggested that they were dispensible. Together, mutational analyses and the conservation of target sites within *Caenorhabditis* and *Drosophila* species support the predictive value of the free energy of sequences flanking true miRNA target sites.

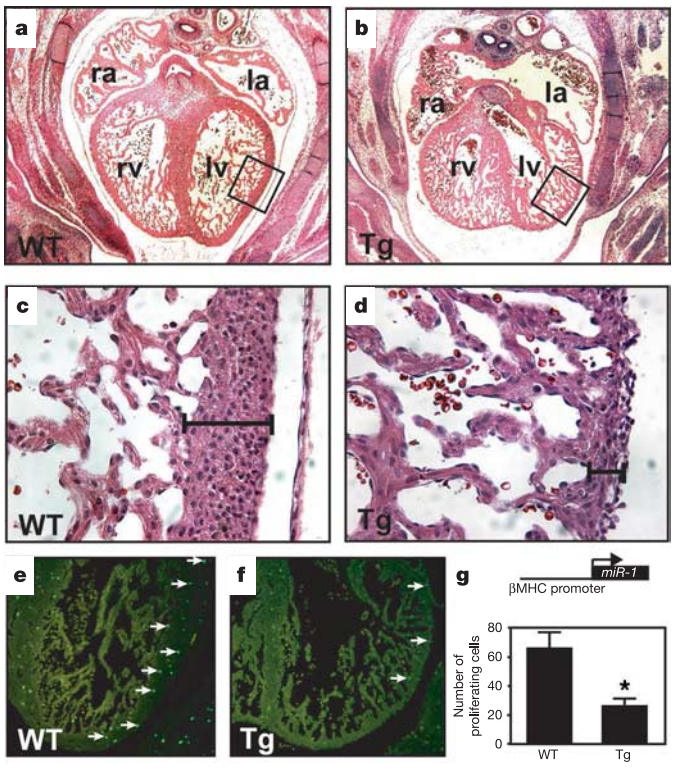

Figure 3 | *miR-1* regulates pool of proliferating ventricular cardiomyocytes and ventricular expansion. **a**–**d**, Transverse sections of wild-type (**a**) or β-MHC-*miR-1* transgenic (**b**) hearts at E13.5. Boxed areas are shown below at higher magnification (**c**, **d**), with the black bar illustrating the narrowed width of the compact layer in transgenic hearts. **e**, **f**, Immunohistochemical staining in wild-type (**e**) and transgenic (**f**) hearts using an antibody specific to phosphohistone H3, to mark proliferating cells. Arrows indicate proliferating cells. **g**, Quantification of cycling cells shows a statistically significant decrease (asterisk) in the number of proliferating cells in *miR-1* transgenic hearts ($n = 3$). Error bars indicate standard deviations. Abbreviations: la, left atrium; lv, left ventricle; ra, right atrium; rv, right ventricle.

In addition to the flanking sequence, we analysed the stability of the predicted miRNA target sequence itself to determine whether we could find RNA structural features that might affect accessibility and enhance the specificity of target prediction. In a simplified view, the secondary structure of RNA can consist of stems, loops or unstructured single strands. Long stems are stabilizing elements that might render the RNA less accessible to miRNAs. All long loops, including hairpin, interior, bulge and multi-branching loops, could be considered destabilizing elements. Unstructured single strands (including joint sequences and free ends) are also destabilizing, and together with other destabilizing elements, might represent structures that permit miRNA and target sequence interaction. We found that no validated target sites contained stabilizing elements, but most target sequences did have destabilizing elements. Several putative sites that had high ΔGs or had been experimentally dispensible also had stabilizing elements. Consistent with this idea, reported mutations in the spacer region between sites I and II in *lin-41* (ref. 10), which abolished miRNA repression, altered the secondary structure and resulted in the loss of destabilizing elements (Table 1 and Supplementary Fig. 2). There were almost no exceptions to the association of stabilizing elements or destabilizing elements with targets, suggesting that the presence or absence of stabilizing elements and destabilizing elements might have predictive value in an *in silico* screen for putative miRNA targets.

On the basis of the above observations, we searched for putative miR-1 targets using several assumptions and criteria (Fig. 4a). First, we searched for mRNAs that were complementary to the first eight nucleotides of miR-1. Second, consistent with recent reports of free energy of binding[42], an A to G switch at the eighth nucleotide gave the strongest ΔG, suggesting that a G–U wobble at this position would be allowed (or possibly preferred) for miR-1 binding to its mRNA targets. Third, we assumed that true 3′-UTR targets would share conservation between chick, mouse, rat and human. Finally, we used mFold to analyse the local mRNA secondary structure 70 bp 5′ and 3′ of the putative miRNA binding site, selecting for instability within the predicted region, and assessed the secondary structure of the target sequence for the presence of stabilizing or destabilizing elements.

Using these criteria, we scanned all known mRNA 3′-UTRs as potential miR-1 targets. Approximately 13 mRNA 3′-UTRs matched miR-1, and the putative target sequences were conserved across species (Fig. 4b). However, most 5′ and 3′ flanking regions had ΔGs that were close to the species average, and did not suggest local instability (Fig. 4b). To validate putative targets and to test whether the ΔG and stabilizing/destabilizing elements would add further specificity to our *in silico* screen, we selected for further study a few predicted targets that were co-expressed with *miR-1* genes in the heart or skeletal muscle. One of these, the transcription factor Hand2 had a particularly unstable 5′ region, with a ΔG of -4.6 kcal mol^{-1}. Animals lacking Hand2 show characteristic failure of ventricular cardiomyocyte expansion[18,20,22,23]. We also tested thymosin β4, a cardioprotective G-actin-sequestering protein expressed during cardiogenesis[43] that does not have a predicted ΔG lower than the average but shows high sequence complementarity with miR-1 (see Supplementary Fig. 3).

Previous studies suggest that miRNA-binding sites are transferable and sufficient for conferring miRNA-dependent translational repression[39,42]. To test this, we placed multimers of about 80 bp containing the predicted miR-1 target site from *Hand2* or thymosin β4 3′-UTRs into the 3′-UTR of a luciferase reporter plasmid (Fig. 4c). We introduced the luciferase expression vector under a constitutively active promoter with or without *miR-1* into COS1 cells and measured the level of luciferase enzyme activity to determine the effects of miR-1 on luciferase translation. Transfection of the *Hand2* chimaeric luciferase reporter into COS1 cells, which do not express any endogenous miR-1 (Fig. 1b), consistently resulted in decreased luciferase activity when wild-type *miR-1* was also transfected

© 2005 Nature Publishing Group

Table 1 | *In silico* analysis of previously described miRNA targets

Organism	miRNA	Target	Site	ΔG for 5′ 70 bp (−kcal mol^{-1})	ΔG for 3′ 70 bp (−kcal mol^{-1})	DSE	SE
C. elegans (avg. $\Delta G = 7.2$)	Lin-4	*lin-14*	I	7.7	3.4	–	–
			II	7.8	1.5	IL	–
			III	2.6	4.2	HL	–
			IV	5.0	8.3	–	–
			V	4.2	10.6	–	–
			VI	9.3	8.7	–	Stem
			VII	3.2	3.0	Joint	–
		Lin-28	I	0.6	10.1	Free end	–
		lin-57	I	10.2	8.2	Joint	–
			II	3.1	4.8	HL	–
	let-7	*lin-41*	I	0.6	7.6	Joint	–
			II	9.4	7.2	MBL	–
			III	6.2	7.2	IL	–
			IV	8.1	6.3	IL	–
			V	5.1	9.4	HL, free end	Stem
			VI	12.4	5.9	HL	Stem
		lin-41 (MT)	I	0.6	4.4	–	–
			II	6.6	7.2	–	–
		daf-12	I	1.6	10.2	IL	–
			II	8.9	1.1	HL, free end	–
		lin-57	I	1.5	3.9	MBL	–
			II	8.1	8.8	–	–
			III	5.9	4.7	Free end	–
			IV	2.3	0.7	MBL	–
			V	0.3	0.1	HL	–
			VI	0.2	0.3	HL, free end	–
			VII	0.7	3.8	Free end	–
			VIII	0.3	9.0	Free end	–
	lsy-6	*cog-1*	I	1.1	1.7	Free end	–
	miR-273	*die-1*	I	3.8	0.3	Free end	–
			II	4.1	5.5	MBL	–
D. melanogaster (avg. $\Delta G = 8.5$)	bantam	Hid	I	3.4	8.6	HL	–
			II	9.5	9.2	HL	–
			III	1.3	4.1	Free end	–
			IV	24.7	19.2	–	–
			V	8.6	7.2	Joint	–
M. musculus (avg. $\Delta G = 13.4$)	miR-196	*Hoxb8*	I	12.8	1.6	HL	–
	miR-375	myotrophin	I	9.2	7.2	–	–

Free energy (ΔG) analysis of sequence flanking each putative target binding site, and description of the destabilizing elements (DSE) or stabilizing elements (SE) within binding sites. HL, hairpin loop; IL, interior loop; MBL, multi-branching loop; MT, mutant.

(Fig. 4d). This was uniformly true for the putative miR-1 target region from the 3′-UTR of mouse, chick, frog or fish, suggesting evolutionary conservation of *Hand2* as a target of miR-1 (Fig. 4d and Supplementary Fig. 4). In this assay, the 3′-UTR of thymosin β4 also resulted in decreased luciferase activity. A mutant target sequence of *Hand2* or thymosin β4 fused to the 3′-UTR of luciferase was not responsive to wild-type miR-1, suggesting specificity of the repression effect. Furthermore, mutant *miR-1* genes (see Supplementary Fig. 4) had no effect on the wild-type target sequences, but could partially repress translation of luciferase transcripts containing the complementary mutant 3′-UTRs (Fig. 4d and Supplementary Fig. 4).

Although the ability of miRNAs to repress translation of chimaeric luciferase reporters is a useful screening tool, it remains a surrogate for testing the effects of miRNAs on their putative targets and can result in misleading assessment of targets. To more directly test the validity of putative targets, we asked whether miR-1 could repress endogenous protein expression *in vivo* in transgenic mice (Supplementary Fig. 5). Western blots of transgenic heart protein overexpressing *miR-1* postnatally showed a significant decrease in Hand2 protein levels compared with non-transgenic littermates, confirming *Hand2* as a miR-1 target *in vivo* (Fig. 4e). No change in mRNA levels of *Hand2* was noted (Fig. 4e). Together, the *in silico*, *in vitro* and *in vivo* data provide compelling evidence that *Hand2* is a true target of miR-1 during cardiogenesis. In contrast, we did not detect any difference in thymosin β4 protein levels in the *miR-1*-overexpressing transgenic hearts compared with wild type, despite perfect sequence complementarity and conservation (Fig. 4e and Supplementary Fig. 3). This is consistent with the regions of high ΔG around the target sequence of thymosin β4. Similarly, despite the low ΔG for another putative target, insulin-like growth factor 1 (*Igf1*), we did not detect any change in IGF1 protein levels in transgenic hearts, consistent with the presence of a stabilizing element in the target sequence (Fig. 4b).

Discussion

Here we have described a conserved cardiac- and skeletal-muscle-specific regulatory pathway involving an SRF–myocardin-dependent miRNA that regulates translation of the central cardiac transcription factor Hand2. The early exit of cardiomyocytes from the cell cycle upon overexpression of *miR-1* might reflect the role of miR-1 downstream of SRF and myocardin, to more finely regulate the balance between cell proliferation and differentiation. The potential role for miR-1 s in mediating the effect of MyoD on skeletal muscle differentiation might be equally important and awaits future studies.

The observation that *miR-1* expression begins after cardiac looping and becomes robust only later is consistent with a model in which temporal regulation of Hand2 activity is necessary for cardiac differentiation. Through regulation of Hand2 (and probably other critical factors), miR-1 s appear to regulate their targets temporally and spatially, contributing to multiple aspects of cardiogenesis. This type of regulation might be common during embryogenesis in order to titrate the effects of critical signalling and transcriptional pathways, and allow appropriate decisions regarding cell fate, proliferation and differentiation.

The algorithm we used to predict miRNA targets is based on observations from previously validated targets and is an attempt to

© 2005 Nature Publishing Group

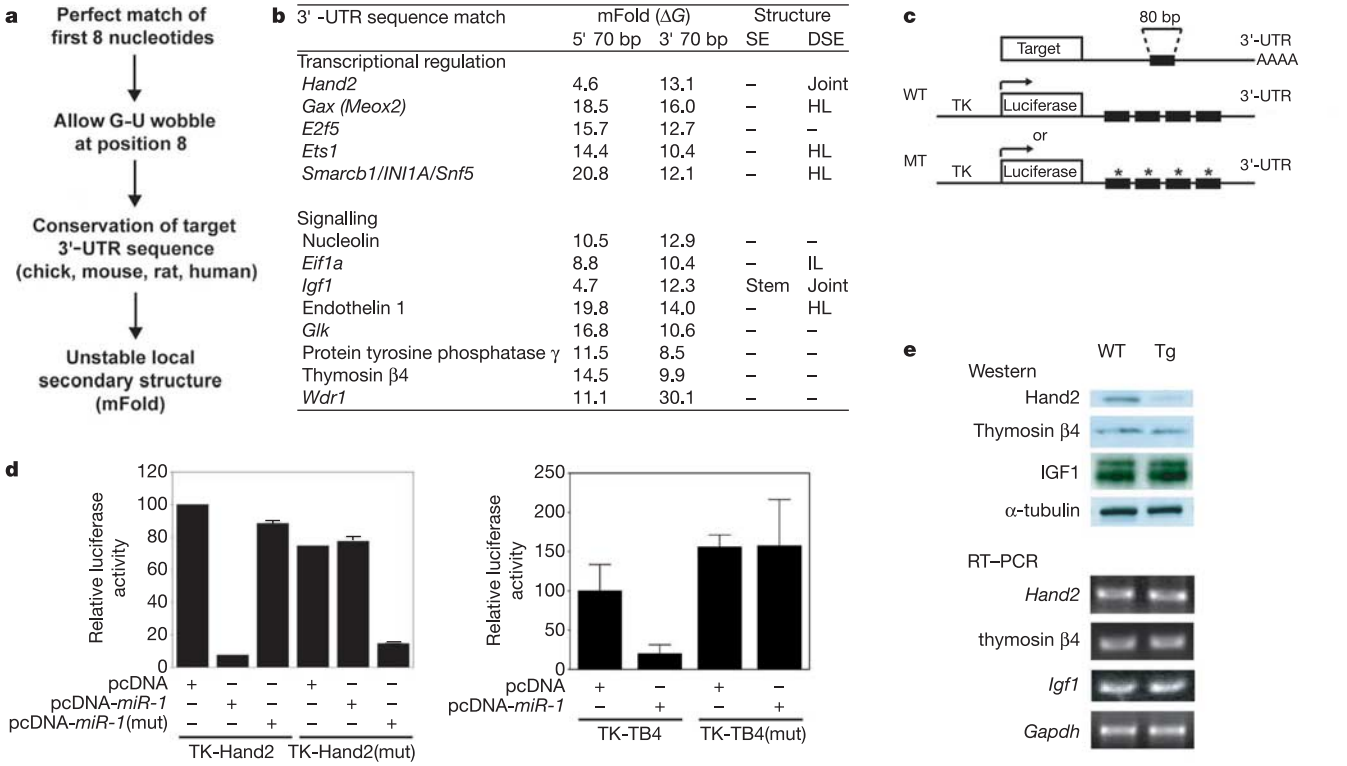

Figure 4 | Prediction and validation of miR-1 targets. a, Algorithm for *in silico* prediction of microRNA targets. **b**, List of mRNA sequences with conserved sequence matching with *miR-1* across species. Predicted ΔG ($-$kcal mol^{-1}) of 70 bp 5′ and 3′ flanking regions neighbouring potential target sites is shown. Presence of stabilizing elements (SE) or destabilizing elements (DSE) in the target sequence structure. **c**, Approach for testing the transferability of the *miR-1* target sequence to the luciferase reporter using multimerized copies of wild-type or mutant (asterisks) sequence. TK, thymidine kinase promoter. **d**, Relative luciferase activity under various conditions using the 3′-UTR target sequence of mouse *Hand2* and the target sequence of thymosin β4 transferred to the luciferase 3′-UTR (TK-Hand2 or TK-TB4, respectively). Error bars indicate standard deviations. **e**, Western blot of protein from wild-type hearts and transgenic hearts overexpressing *miR-1*. RNA transcript levels were equal, as seen by RT–PCR (bottom panel).

develop certain 'principles' that appear to be followed by known miRNAs and their targets[4–11,39,40,44]. The major difference between our approach and that of others is the additional evaluation of the energy states of sequences flanking the miRNA target (ΔG) and the presence or absence of stabilizing/destabilizing elements in target RNA. Consistent with RNA secondary structure having an important role in miRNA target accessibility, ATP-assisted unwinding of RNA secondary structure does not seem to be involved in target recognition by short interfering (si)RNA[45,46]. We propose a model in which miRNAs preferentially target 3′-UTR regions with less complex secondary structure that are more accessible. The criteria described here may lead to increased specificity of target prediction, perhaps at the expense of sensitivity. Formal testing of this model will be possible as additional, biologically validated microRNA targets are identified.

METHODS

Bioinformatics. Multiple sequence alignment was performed with ClustalX 1.83 using appropriate settings, and promoter analysis was performed with rVISTA. PatScan[47] program was used for target searches, and energy states and RNA folding were determined using mFold[48]. Average ΔG values in each species were determined by randomly selecting 60 3′-UTR fragments of 70 bp in length.

We determined the RNA secondary structure of each miRNA-binding site plus 30 bp flanking sequence on each side. On the basis of our observations, we set the following values as a cutoff to define stabilizing and destabilizing elements. Average stem length was calculated for each species from at least 60 randomly selected sequences, and cutoff for a stabilizing element stem was defined as: ≥8 bp (worms), ≥9 bp (flies), ≥10 bp (mice). Loops or unstructured single strands were defined as destabilizing elements with the following cutoff lengths: hairpin loop, ≥11 bp; interior loop, ≥9 bp; bulge loop, ≥7 bp; multiple-branching loop, ≥11 bp; joint sequence and free end, ≥11 bp.

Plasmid construction. Target sequences and their mutant forms were synthesized as DNA oligonucleotides. After annealing and concatamerization, four copies of the target sequence were excised using a sized gel, blunt ended and subcloned into a pGL-TK vector. To express *miR-1* genes in COS1 cells, the genomic sequence containing pre-*miR-1* gene sequences plus about 50 bp flanking each side were inserted into pcDNA3. Site-directed mutagenesis by polymerase chain reaction (PCR) was performed using Pfu DNA polymerase.

Cell transfection, EMSA, luciferase assay, northern and western blotting. Plasmid transfection was performed in 12-well plates using FuGENE 6 (Roche). An RSV-lacZ expression construct was co-transfected to normalize for transfection efficiency. Luciferase and β̃-galactosidase activities in the cell extract were assayed 36 h after transfection using a luciferase assay system (Promega). All experiments were repeated at least three times, and representative results are shown. Northern blotting was performed as previously described[25]. Western blotting was performed on heart lysates using standard methods with specific antibodies. Electrophoretic mobility-shift assays (EMSA) were performed as previously described[49].

Transgenic mice. Transgenic mice were generated and β-galactosidase staining and histological analyses were performed as previously described[49]. For promoter analysis, different fragments were subcloned into a pHsp68lacZ reporter vector. For overexpression studies, pre-*miR-1* plus flanking sequence was subcloned into α-MHCclone26 or β-MHCclone32 vectors.

Received 7 March; accepted 17 May 2005.
Published online 12 June 2005.

1. He, L. & Hannon, G. J. MicroRNAs: small RNAs with a big role in gene regulation. *Nature Rev. Genet.* **5**, 522–531 (2004).
2. Ambros, V. The functions of animal microRNAs. *Nature* **431**, 350–355 (2004).
3. Meister, G. & Tuschl, T. Mechanisms of gene silencing by double-stranded RNA. *Nature* **431**, 343–349 (2004).
4. Lee, R. C., Feinbaum, R. L. & Ambros, V. The *C. elegans* heterochronic gene lin-4 encodes small RNAs with antisense complementarity to lin-14. *Cell* **75**, 843–854 (1993).

© 2005 Nature Publishing Group

5. Wightman, B., Ha, I. & Ruvkun, G. Posttranscriptional regulation of the heterochronic gene lin-14 by lin-4 mediates temporal pattern formation in *C. elegans*. *Cell* **75,** 855–862 (1993).
6. Moss, E. G., Lee, R. C. & Ambros, V. The cold shock domain protein LIN-28 controls developmental timing in *C. elegans* and is regulated by the *lin-4* RNA. *Cell* **88,** 637–646 (1997).
7. Brennecke, J., Hipfner, D. R., Stark, A., Russell, R. B. & Cohen, S. M. *bantam* encodes a developmentally regulated microRNA that controls cell proliferation and regulates the proapoptotic gene *hid* in *Drosophila*. *Cell* **113,** 25–36 (2003).
8. Abrahante, J. E. *et al.* The *Caenorhabditis elegans hunchback*-like gene *lin-57/hbl-1* controls developmental time and is regulated by microRNAs. *Dev. Cell* **4,** 625–637 (2003).
9. Johnston, R. J. & Hobert, O. A microRNA controlling left/right neuronal asymmetry in *Caenorhabditis elegans*. *Nature* **426,** 845–849 (2003).
10. Vella, M. C., Choi, E. Y., Lin, S. Y., Reinert, K. & Slack, F. J. The *C. elegans* microRNA *let-7* binds to imperfect *let-7* complementary sites from the *lin-41* 3′UTR. *Genes Dev.* **18,** 132–137 (2004).
11. Chang, S., Johnston, R. J. Jr, Frokjaer-Jensen, C., Lockery, S. & Hobert, O. MicroRNAs act sequentially and asymmetrically to control chemosensory laterality in the nematode. *Nature* **430,** 785–789 (2004).
12. Chien, K. R. & Olson, E. N. Converging pathways and principles in heart development and disease: CV@CSH. *Cell* **110,** 153–162 (2002).
13. Srivastava, D. & Olson, E. N. A genetic blueprint for cardiac development. *Nature* **407,** 221–226 (2000).
14. Norman, C., Runswick, M., Pollock, R. & Treisman, R. Isolation and properties of cDNA clones encoding SRF, a transcription factor that binds to the c-fos serum response element. *Cell* **55,** 989–1003 (1988).
15. Miralles, F., Posern, G., Zaromytidou, A. I. & Treisman, R. Actin dynamics control SRF activity by regulation of its coactivator MAL. *Cell* **113,** 329–342 (2003).
16. Shin, C. H. *et al.* Modulation of cardiac growth and development by HOP, an unusual homeodomain protein. *Cell* **110,** 725–735 (2002).
17. Chen, F. *et al. Hop* is an unusual homeobox gene that modulates cardiac development. *Cell* **110,** 713–723 (2002).
18. Yelon, D. *et al.* The bHLH transcription factor Hand2 plays parallel roles in zebrafish heart and pectoral fin development. *Development* **127,** 2573–2582 (2000).
19. Srivastava, D., Cserjesi, P. & Olson, E. N. A subclass of bHLH proteins required for cardiac morphogenesis. *Science* **270,** 1995–1999 (1995).
20. Srivastava, D. *et al.* Regulation of cardiac mesodermal and neural crest development by the bHLH transcription factor, dHAND. *Nature Genet.* **16,** 154–160 (1997).
21. Firulli, A. B., McFadden, D. G., Lin, Q., Srivastava, D. & Olson, E. N. Heart and extra-embryonic mesodermal defects in mouse embryos lacking the bHLH transcription factor Hand1. *Nature Genet.* **18,** 266–270 (1998).
22. Yamagishi, H. *et al.* The combinatorial activities of Nkx2.5 and dHAND are essential for cardiac ventricle formation. *Dev. Biol.* **239,** 190–203 (2001).
23. McFadden, D. G. *et al.* The Hand1 and Hand2 transcription factors regulate expansion of the embryonic cardiac ventricles in a gene dosage-dependent manner. *Development* **132,** 189–201 (2005).
24. Wang, D. *et al.* Activation of cardiac gene expression by myocardin, a transcriptional cofactor for serum response factor. *Cell* **105,** 851–862 (2001).
25. Lee, R. C. & Ambros, V. An extensive class of small RNAs in *Caenorhabditis elegans*. *Science* **294,** 862–864 (2001).
26. Lagos-Quintana, M., Rauhut, R., Lendeckel, W. & Tuschl, T. Identification of novel genes coding for small expressed RNAs. *Science* **294,** 853–858 (2001).
27. Kelly, R. G. & Buckingham, M. E. The anterior heart-forming field: voyage to the arterial pole of the heart. *Trends Genet.* **18,** 210–216 (2002).
28. Miano, J. M. *et al.* Restricted inactivation of serum response factor to the cardiovascular system. *Proc. Natl Acad. Sci. USA* **101,** 17132–17137 (2004).
29. Wang, Z. *et al.* Myocardin and ternary complex factors compete for SRF to control smooth muscle gene expression. *Nature* **428,** 185–189 (2004).
30. Wang, D. Z. & Olson, E. N. Control of smooth muscle development by the myocardin family of transcriptional coactivators. *Curr. Opin. Genet. Dev.* **14,** 558–566 (2004).
31. Zhou, J. & Herring, B. P. Mechanisms responsible for the promoter-specific effects of myocardin. *J. Biol. Chem.* **280,** 1086–1089 (2005).
32. Lai, E. C. Micro RNAs are complementary to 3′ UTR sequence motifs that mediate negative post-transcriptional regulation. *Nature Genet.* **30,** 363–364 (2002).
33. Stark, A., Brennecke, J., Russell, R. B. & Cohen, S. M. Identification of *Drosophila* microRNA targets. *PLoS Biol.* **1,** E60 (2003).
34. Lewis, B. P., Shih, I. H., Jones-Rhoades, M. W., Bartel, D. P. & Burge, C. B. Prediction of mammalian microRNA targets. *Cell* **115,** 787–798 (2003).
35. Kiriakidou, M. *et al.* A combined computational-experimental approach predicts human microRNA targets. *Genes Dev.* **18,** 1165–1178 (2004).
36. John, B. *et al.* Human MicroRNA targets. *PLoS Biol.* **2,** e363 (2004).
37. Lewis, B. P., Burge, C. B. & Bartel, D. P. Conserved seed pairing, often flanked by adenosines, indicates that thousands of human genes are microRNA targets. *Cell* **120,** 15–20 (2005).
38. Rhoades, M. W. *et al.* Prediction of plant microRNA targets. *Cell* **110,** 513–520 (2002).
39. Yekta, S., Shih, I. H. & Bartel, D. P. MicroRNA-directed cleavage of HOXB8 mRNA. *Science* **304,** 594–596 (2004).
40. Poy, M. N. *et al.* A pancreatic islet-specific microRNA regulates insulin secretion. *Nature* **432,** 226–230 (2004).
41. Lee, N. S. *et al.* Expression of small interfering RNAs targeted against HIV-1 *rev* transcripts in human cells. *Nature Biotechnol.* **20,** 500–505 (2002).
42. Doench, J. G. & Sharp, P. A. Specificity of microRNA target selection in translational repression. *Genes Dev.* **18,** 504–511 (2004).
43. Bock-Marquette, I., Saxena, A., White, M. D., Dimaio, J. M. & Srivastava, D. Thymosin β4 activates integrin-linked kinase and promotes cardiac cell migration, survival and cardiac repair. *Nature* **432,** 466–472 (2004).
44. Grosshans, H., Johnson, T., Reinert, K. L., Gerstein, M. & Slack, F. J. The temporal patterning microRNA *let-7* regulates several transcription factors at the larval to adult transition in *C. elegans*. *Dev. Cell* **8,** 321–330 (2005).
45. Haley, B. & Zamore, P. D. Kinetic analysis of the RNAi enzyme complex. *Nature Struct. Mol. Biol.* **11,** 599–606 (2004).
46. Doench, J. G., Petersen, C. P. & Sharp, P. A. siRNAs can function as miRNAs. *Genes Dev.* **17,** 438–442 (2003).
47. Dsouza, M., Larsen, N. & Overbeek, R. Searching for patterns in genomic data. *Trends Genet.* **13,** 497–498 (1997).
48. Zuker, M. Mfold web server for nucleic acid folding and hybridization prediction. *Nucleic Acids Res.* **31,** 3406–3415 (2003).
49. Yamagishi, H. *et al. Tbx1* is regulated by tissue-specific forkhead proteins through a common Sonic hedgehog-responsive enhancer. *Genes Dev.* **7,** 269–281 (2003).

Supplementary Information is linked to the online version of the paper at www.nature.com/nature.

Acknowledgements We wish to thank K. Ivey for critical discussions and for preparation of figures; members of the Srivastava laboratory for helpful discussions; J. McAnally for generation of transgenic mice; E. N. Olson for plasmids; and R. Misra and R. Balza for providing SRF-null embryonic heart cDNA. D. S. was supported by grants from NHLB/NIH, the March of Dimes Birth Defects Foundation and the American Heart Association.

Author Information MicroRNA 1 sequences have been deposited in Genbank under the following accession numbers: DQ066648 and DQ 066649 (*Pan troglodytes* pre-microRNA-1-1 and 1-2), DQ066650 (rat pre-microRNA-1), DQ066651 (*Danio rerio* pre-microRNA-1) and DQ066652 (*Xenopus tropicalis* pre-microRNA-1). Reprints and permissions information is available at npg.nature.com/reprintsandpermissions. The authors declare no competing financial interests. Correspondence and requests for materials should be addressed to D.S. (dsrivastava@gladstone.ucsf.edu).

© 2005 Nature Publishing Group